



CRACK DETECTION IN A ROTOR DYNAMIC SYSTEM BY VIBRATION MONITORING

Dr.Nabil H. H.
Univ. of Baghdad
College of Eng.

Jawad K.Z.
Univ. of Baghdad
College of Eng.

ABSTRACT.

Vibration monitoring is one of the most important techniques which are used to detect the cracks or defects in rotating mechanical systems. To distinguish characteristics of the system response that may lead to the transverse crack in rotating shaft, local asymmetry crack model is used where crack simulated by increasing the flexibility of the shaft and transverse crack in the shaft is introduced.

The obtained results showed a decreasing in the resonance shaft speed with increasing the crack depth ratio. The feature is used for diagnostics the crack in the shaft by using the graphed results between the natural frequency and shaft speed. The method of detecting was applied for several crack depth ratios (uncracked, %10, %20 and %30) in a clamped-free rotor. Also for investigating the effect of position of crack and effect of mass location, a crack and mass with different locations are introduced in the shaft. Although, the presence of a transverse shaft crack has also been shown to induce an unstable response for some shaft speeds and the behavior of the 2x harmonic component of the system response is effective target observation for a monitoring system.

الخلاصه:

اكتشاف الشقوق او العيوب في الانظمة الديناميكية الدواره من خلال مراقبة الاهتزازات يعتبر ذو اهميه كبيره وقد استخدمت في عملية التحليل هذه نموذجين هما نموذج لشق شامل على طول العمود والاخرنموذج لشق موقعي اي في مكان محدد من العمود وذلك لغرض تحديد صفات استجابة النظام والتي تدلل على وجود شق عرضي في العمود وان هذا التحليل طبق على نوعين من الاعمده الدواره من حيث الشروط الحدوديه هما (Simply-Supported) و (Free) ولاعماق مختلفه (0% , 10% و 20% , 30%) من قطر اعمود حيث تم تمثيل الشق بزياده في مرونة العمود الدوار . كذلك بينت النتائج بوجود الشق يكون النظام غير مستقر عند سرع دوارانيه معينه.

KEYWORDS: Vibration, Rotor, Crack Detection, transverse crack, flexibility, resonance shaft speed.

INTRODUCTION:

This research deals with detection of crack in clamped-free and simply-supported rotors by using of the resonance shaft speed. The magnitude of the crack depth will be determined by measuring the natural frequency of the rotor.

A uniform transverse crack, located on clamped-free and simply-support rotors of a circular cross-section which will be used as the physical model of the system. The crack on the shaft is assumed to be open during the transverse vibration of the rotor. This assumption will permit the effect of closing and opening of the crack in the analysis to be ignored.

An uncracked shaft has constant stiffness and has a constant displacement under a fixed load regardless of the angle of rotation. In cracked shaft, the cracked portion of the cross-section is not capable of supporting a tensile stress. Therefore, the displacement, as a function of the stiffness, is minimum when the crack is closed and maximum when the crack is open. This opening and closing behavior, which is referred to as "breathing", results in time dependent stiffness coefficients in the equation of motion of the system, which is difficult to work with. Obtaining solutions usually requires making broad simplifying assumption or some type of numerical approximation.

System in which the displacements and vibration amplitudes remain very small result in a crack that remains essentially open regardless, of the angle of rotation. This type of crack, which is essentially a local stiffness asymmetry, is referred to as a "gaping" crack. The analysis of systems containing a gaping crack is extremely useful since the response characteristics, on crack indicators, identified in the gaping crack analysis are also present in the analysis of systems containing a breathing crack. Furthermore, these indicators prove to be the most practical, in terms of implementation, in the detection of real cracks. Also, since the introduction of a crack into a rotating system, on the most basic level, results in a system with a stiffness asymmetry, the analysis of systems containing an asymmetry is fundamental to the study of the dynamics of cracked rotating systems.

The primary effect of the presence of a crack in a rotating shaft is clearly a local reduction in stiffness. This highly localized effect does not influence the stiffness of the regions of the rotor away from the cracked cross section. Regardless of the type of cracked model used for analysis, the effective overall stiffness of the rotor is no longer symmetric. The analysis of the response of a rotor with designed-in asymmetry is therefore part of the fundamental basis for the analysis of the dynamic of shaft containing a transverse crack. It is important to note that for rotating systems the terms "natural frequency" and "whirl-frequency" are synonymous. Also, the terms "critical speed" refers to a shaft speed for which one or more of the natural (whirl) frequencies of the system are equal to the shaft speed. Therefore, the maximum 2x harmonic response occurs at shaft speeds that are approximately one-half of a critical speed, i.e. $1/2 n_{cr}$.

In summery, the introduction of a gaping crack model into an existing system model has been shown to be a very effective method of obtaining reasonably accurate results from analysis, yet it avoids the inherent complexities of cracked shaft analysis due to breathing behavior. A discrete representation of the system allows the additional flexibility due to the crack to be placed arbitrarily along the axis of the shaft of the system. The 2x harmonic component of the system response is clearly the most practically implemented indicator for a monitoring and detection system.

LOCAL MODEL OF CRACKED ROTATING SHAFT

The presence of transverse crack in a rotating shaft introduces highly localized flexibility. The additional flexibility that resulting from presence of crack must be determined and incorporated this flexibility into a discrete representation of the system. To achieve this localizing effect a transfer matrix method was used. The following are the general data table (1.1) for rotor in local model which was used for crack detection.

Table (1.1) rotor data, local model

Length	0.5m
Diameter	0.1m
Density	7850 kg/m ³
Modules of elasticity (E)	200E9 N/m ²
Crack depth (a)	Uncracked, 0.1D, 0.2D, 0.3D,
Poisson ratio (ν)	0.3
Shaft speed (n)	125 Hz

Figure 1.1 shows the three lumped stiffness elements; $[F_1]$, $[F_{crack}]$ and $[F_2]$, and the three lumped inertia elements; $[ms_1]$, $[ms_2]$ and $[P]$ for a cracked system.

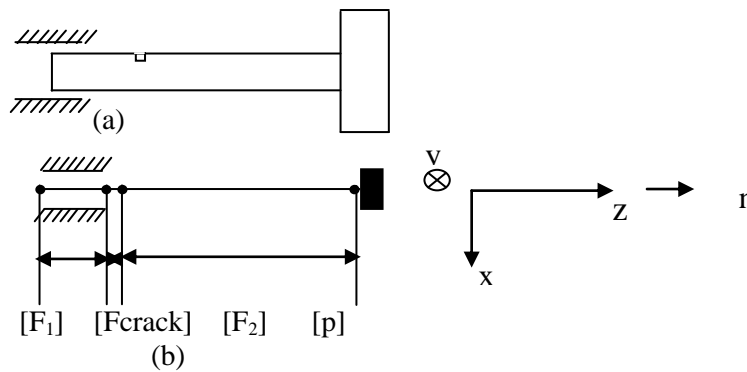
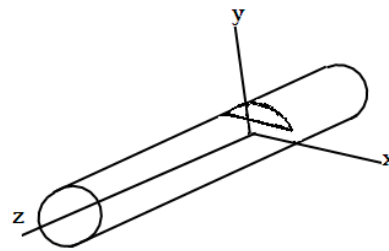


Figure (1.1) Local Model

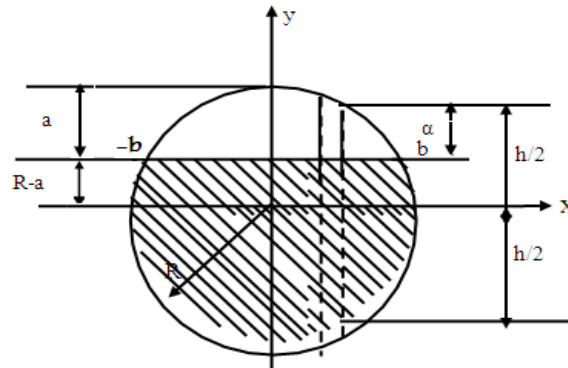
In this section we will use the Extended Transfer Matrix Method as by A.S. Lee and I. Green (1994) and by E.C. Pestel and F.A. Leckie. (1963) for free response analysis.

Local Flexibility Matrix of Cracked Circular Cross- Section Shaft.

A crack on an elastic shaft introduces a local flexibility that affects the dynamic response of the system and its stability. To establish the local flexibility matrix of the cracked shaft under general loading, a shaft with a transverse crack is considered as shown in figure 1.2a. The crack has a uniform depth a along $-y$ -axis and the shaft loaded with an axial forces P_1 , transverse shear load P_2 & P_3 , bending moment P_4 & p_5 and torsion moment p_6



(a) Shaft Containing Crack



(b) Cross-Section Crack

Figure 1.2: cross-section of the cracked shaft at the location of the crack.

The additional displacement u_i along the direction of loading p_i and U the strain energy due to the crack are related by Castigliano's theorem as follow

$$u_i = \frac{\partial U}{\partial P_i} \quad (1.7)$$

where U has the form:-

$$U = \int_0^{\alpha} J(\alpha) d\alpha \quad (1.8)$$

therefore

$$u_i = \frac{\partial}{\partial P_i} \int_0^{\alpha} J(\alpha) d\alpha \quad (1.9)$$

Where P_i is the generalized force associated with u_i and $J(\alpha)$ is the strain energy density function according to Nikpour and Diamarogones (1988) given by :

$$J(\alpha) = E' \left[\left(\sum_{i=1}^6 K_{Ii} \right)^2 + \left(\sum_{i=1}^6 K_{IIi} \right)^2 + (1 + \nu) \left(\sum_{i=1}^6 K_{IIIi} \right)^2 \right] dy dx \quad (1.10)$$

where:- $E' = \frac{1-\nu^2}{E}$ for plane strain

E: Young's Modulus

ν : Poisson's ratio

K_{ni} : crack stress intensity factor for mode n due to the type of applied load i.

In general the stress intensity factor (SIF) K_{ni} ($n=1,11,111$) can not be taken as the same formats as the counterparts of isotropic material with the same geometry and loading. The SIFs, K_{ni} for a unit width strip of depth α is obtained as follow:-

$$K_{ni} = \sigma_i \sqrt{\pi\alpha} F_n \left(\frac{\alpha}{h} \right) \tag{1.11}$$

where:-

σ_i : stress due to the load P_i

$F_n \left(\frac{\alpha}{h} \right)$ the correction function

h: total length for the strip

the local flexibility matrix $[C_{ij}]$ per unit width has the components

$$C_{ij} = \frac{\partial^2}{\partial P_i \partial P_j} \int_0^\alpha J(\alpha) d\alpha \tag{1.12}$$

after integration equation 4.12 along the crack edge length from b to (-b) becomes :-

$$C_{ij} = \frac{\partial^2}{\partial P_i \partial P_j} \iint J(\alpha) dy dx \tag{1.13}$$

Substitution of equation (4.10) into (4.12) yields:

$$C_{ij} = \frac{\partial^2}{\partial P_i \partial P_j} \iint_{-b}^b \frac{1-\nu^2}{E} \left[\left(\sum_{i=1}^6 KI_i \right)^2 + \left(\sum_{i=1}^6 KII_i \right)^2 + (1+\nu) \left(\sum_{i=1}^6 KIII_i \right)^2 \right] dy dx \tag{1.14}$$

Based on equations (4.11) the components of interest in the local flexibility matrix C_{ij} become:

$$c_{11} = 0 \quad , \quad c_{12} = 0 \quad , \quad c_{23} = c_{32} = 0$$

$$c_{22} = \frac{4(1-\nu^2)}{\pi ER} \int_0^{\frac{b}{R}} \int_0^{\frac{a}{R}} \frac{Y}{R} F_{111}^2 \left(\frac{Y}{R}, \frac{X}{R} \right) d\left(\frac{Y}{R}\right) d\left(\frac{X}{R}\right) \tag{1.15}$$

$$c_{33} = \frac{4(1-\nu^2)}{\pi ER} \int_0^{\frac{b}{R}} \int_0^{\frac{a}{R}} \frac{Y}{R} F_{111}^2 \left(\frac{Y}{R}, \frac{X}{R} \right) d\left(\frac{Y}{R}\right) d\left(\frac{X}{R}\right) \tag{1.16}$$

$$c_{44} = \frac{32(1-\nu^2)}{\pi ER^3} \int_0^{\frac{b}{R}} \int_0^{\frac{a}{R}} \left(\frac{X}{R}\right)^2 \left(\frac{Y}{R}\right) F_{1y}^2 \left(\frac{Y}{R}, \frac{R}{h}\right) d\left(\frac{Y}{R}\right) d\left(\frac{X}{R}\right) \quad (1.17)$$

$$c_{45} = c_{54} = \frac{64(1-\nu^2)}{\pi ER^3} \int_0^{\frac{b}{R}} \int_0^{\frac{a}{R}} \left(\frac{x}{R}\right) \left(\frac{Y}{R}\right) \sqrt{1-\left(\frac{\alpha}{R}\right)^2} F_{1x} \left(\frac{Y}{R}, \frac{R}{h}\right) F_{1y} \left(\frac{y}{R}, \frac{R}{h}\right) d\left(\frac{y}{R}\right) d\left(\frac{X}{R}\right)$$

$$c_{55} = \frac{64(1-\nu^2)}{\pi ER^3} \int_0^{\frac{b}{R}} \int_0^{\frac{a}{R}} \left\{1-\left(\frac{\alpha}{R}\right)^2\right\} \left(\frac{Y}{R}\right) F_{1x}^2 \left(\frac{Y}{R}, \frac{R}{h}\right) d\left(\frac{Y}{R}\right) d\left(\frac{X}{R}\right) \quad (1.18)$$

(1.19)

Where: $F_{III}\left(\frac{\alpha}{h}\right) = \sqrt{\frac{\tan \lambda}{\lambda}}$

$$F_{II}\left(\frac{\alpha}{h}\right) = \left[1.122 - 0.561\left(\frac{\alpha}{h}\right) + 0.85\left(\frac{\alpha}{h}\right)^2 + 0.18\left(\frac{\alpha}{h}\right)^3\right] \sqrt{1-\frac{\alpha}{h}}$$

$$F_{1y}\left(\frac{\alpha}{h}\right) = \sqrt{\frac{\tan \lambda}{4P_1^2}} \left[0.752 + 2.02\left(\frac{\alpha}{h}\right) + 0.37(1-\sin \lambda)^3\right] / \cos \lambda$$

$$\sigma_1 = \frac{\pi d^2}{\pi d^2}$$

$$KI_4 = \sigma_4 \sqrt{\pi \alpha} F_6\left(\frac{\alpha}{h}\right)$$

$$\lambda = \left(\frac{\pi \alpha}{2h}\right)$$

$$\sigma_4 = \frac{32P}{\pi d^2}$$

In dimensionless form.

$$C_{22} = c_{22} \frac{\pi ER}{1-\nu^2}$$

$$C_{33} = c_{33} \frac{\pi ER}{1-\nu^2}$$

$$C_{55} = c_{55} \frac{\pi ER^3}{1-\nu^2}$$

$$C_{45} = c_{45} \frac{\pi ER^3}{1-\nu^2}$$

$$C_{44} = c_{44} \frac{\pi ER^3}{1-\nu^2}$$

} (1.20)

For each crack depth ratio (0%-50%) of the shaft diameter the flexibilities are numerically evaluated, with a program coded in Maple version 7.

These integral expressions are a function of a/D and plotted in figure (1.3).

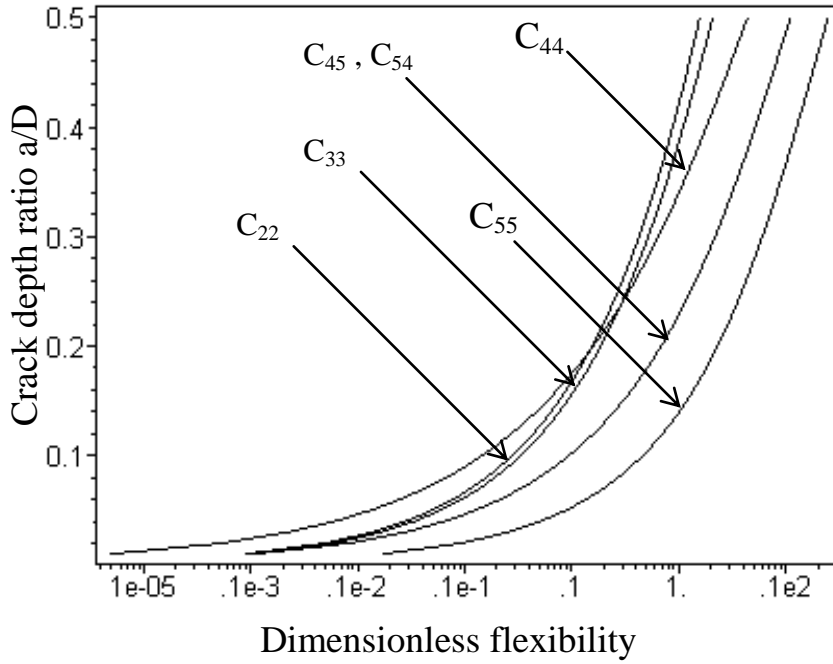


Figure (1.3): Dimensionless Crack Flexibility

Here, the torsion and axial loading is ignored to avoid the coupling therefore the final flexibility at the location of crack which is represented a field matrix may be written as:

$$[F_{crack}] = \begin{bmatrix} 1 & 0 & 0 & -c_{22} & 0 & 0 & 0 & 0 \\ 0 & 1 & c_{44} & 0 & 0 & 0 & c_{45} & 0 \\ 0 & 0 & 1 & 0 & 0 & 0 & 0 & 0 \\ 0 & 0 & 0 & 1 & 0 & 0 & 0 & 0 \\ 0 & 0 & 0 & 0 & 1 & 0 & 0 & -c_{33} \\ 0 & 0 & c_{54} & 0 & 0 & 1 & c_{55} & 0 \\ 0 & 0 & 0 & 0 & 0 & 0 & 1 & 0 \\ 0 & 0 & 0 & 0 & 0 & 0 & 0 & 1 \end{bmatrix} \quad (1.21)$$

TRANSFER MATRIX

Transfer matrix (point matrix and field matrix) relate the state vectors at the ends of the shaft. The state vector at any station may be defined in xyz coordinate system as:

$$\{S\} = \{u_x \quad \theta_y \quad M_y \quad -V_x \quad -u_y \quad \theta_x \quad M_x \quad V_y\}^T \quad (1.22)$$

- As mentioned before.
- u: displacement (m)
- θ: angle (rad)
- V: shear force (N)
- M: moment (N.m)

The field matrix F_i which has the form shown in equation (3.13) is related the state vector at the left $\{S\}_i^L$ to the state vector at right $\{S\}_{i-1}^R$ as following:

$$\{S\}_i^l = [F_i] \{S\}_{i-1}^R \quad (1.23)$$

while the state vector at the left of the station $\{S\}_i^l$ is related to the state at the right lumped mass $\{S\}_i^R$ by the point matrix $[P_i]$

$$\{S\}_i^R = [P] \{S\}_i^l \quad (1.24)$$

OVERALL TRANSFER MATRIX

The overall transfer matrix is found according to:

$$[U] = [P] [\text{shaft}_2] [F_{\text{crack}}] [\text{shaft}_1] \quad (1.25)$$

where:

[U]: Overall transfer matrix

[P]: Point matrix of the attached mass

[F_{crack}]: Crack flexibility matrix

[shaft₁] = [M_{S1}] [F₁]

[shaft₂] = [M_{S2}] [F₂]

M_{S1}, M_{S2}: Point matrix of part one and two of the shaft respectively [left and right of the crack]

F₁, F₂ = Field matrix of the two parts of the shaft.

The state vector at the left side $\{S\}_i^l$ is related to the state vector at the right $\{S\}_i^R$ by the following relation

$$\{S\}_i^R = [U] \{S\}_i^l \quad (1.26)$$

This equation can be solved for different boundary conditions at the left and right ends.

UNDAMPED FREE RESPONSE

clamped – free rotor

In this case the boundary conditions are no displacement or tilt at the support end and no shear or moment at the free end. Applying these conditions to the overall transfer matrix given in equation (4.26) leads to the following:

$$\begin{pmatrix} u_x \\ \theta_y \\ 0 \\ 0 \\ -u_y \\ \theta_y \\ 0 \\ 0 \end{pmatrix}^R = \begin{bmatrix} U_{11} & U_{12} & U_{13} & U_{14} & U_{15} & U_{16} & U_{17} & U_{18} \\ U_{21} & U_{22} & U_{23} & U_{24} & U_{25} & U_{26} & U_{27} & U_{28} \\ U_{31} & U_{32} & U_{33} & U_{34} & U_{35} & U_{36} & U_{37} & U_{38} \\ U_{41} & U_{42} & U_{43} & U_{44} & U_{45} & U_{46} & U_{47} & U_{48} \\ U_{51} & U_{52} & U_{53} & U_{54} & U_{55} & U_{56} & U_{57} & U_{58} \\ U_{61} & U_{62} & U_{63} & U_{64} & U_{65} & U_{66} & U_{67} & U_{68} \\ U_{71} & U_{72} & U_{73} & U_{74} & U_{75} & U_{76} & U_{77} & U_{78} \\ U_{81} & U_{82} & U_{83} & U_{84} & U_{85} & U_{86} & U_{87} & U_{88} \end{bmatrix} \begin{pmatrix} 0 \\ 0 \\ M_y \\ -V_x \\ 0 \\ 0 \\ M_x \\ V_y \end{pmatrix} \text{damped}$$



$$\begin{Bmatrix} 0 \\ 0 \\ 0 \\ 0 \end{Bmatrix}_i^R = \begin{bmatrix} U33 & U34 & U37 & U38 \\ U43 & U44 & U47 & U48 \\ U73 & U74 & U77 & U78 \\ U83 & U84 & U87 & U88 \end{bmatrix} \begin{Bmatrix} M_y \\ -V_x \\ M_x \\ V_y \end{Bmatrix}$$

$$\begin{Bmatrix} 0 \\ 0 \\ 0 \\ 0 \end{Bmatrix}_i^R = [F3] \begin{Bmatrix} M_y \\ -V_x \\ M_x \\ V_y \end{Bmatrix} \tag{1.27}$$

Where:

$$[F3] = \begin{bmatrix} U33 & U34 & U37 & U38 \\ U43 & U44 & U47 & U48 \\ U74 & U74 & U77 & U78 \\ U83 & U84 & U87 & U88 \end{bmatrix}$$

$$\begin{Bmatrix} u_x \\ \theta_y \\ -u_y \\ \theta_y \end{Bmatrix}_i^R = \begin{bmatrix} U13 & U14 & U17 & U18 \\ U23 & U24 & U27 & U28 \\ U53 & U54 & U57 & U58 \\ U63 & U64 & U67 & U68 \end{bmatrix} \begin{Bmatrix} M_y \\ -V_x \\ M_x \\ V_y \end{Bmatrix}_{clamped}$$

$$\begin{Bmatrix} u_x \\ \theta_y \\ -u_y \\ \theta \end{Bmatrix}_i = [F4] \begin{Bmatrix} M_y \\ -V_x \\ M_x \\ V_y \end{Bmatrix} \tag{1.28}$$

Where:

$$[F4] = \begin{bmatrix} U13 & U14 & U17 & U18 \\ U23 & U24 & U27 & U28 \\ U53 & U54 & U57 & U58 \\ U63 & U64 & U67 & U68 \end{bmatrix}$$

RESULTS:

By solving the eigenvalue problem of equation (1.27) four complex conjugate pairs of eigenvalues results and from which obtains the mode shape for a given eigenvalue which is the displacement and till portion of the state vector at the free end of the shaft.

From equation (1.28), the shear and moment portion of the state vector at the clamped is given by:

$$\begin{Bmatrix} M \\ -V_x \\ M_x \\ V_y \end{Bmatrix}_{clamped} = [F4]^{-1} \begin{Bmatrix} u_x \\ \theta_y \\ -u_y \\ \theta_x \end{Bmatrix}_i^R \tag{1.29}$$

Substitution this expression for $\{M_y \quad -V_x \quad M_x \quad V_y\}_{Clamped}$ into equation (4.27) results in:

$$[F_3][F_4]^{-1} \begin{Bmatrix} u_x \\ \theta_y \\ -u_y \\ \theta_x \end{Bmatrix}_i^R = \begin{Bmatrix} 0 \\ 0 \\ 0 \\ 0 \end{Bmatrix} \quad (1.30)$$

Change of natural frequency versus depth of crack ratio also graphed for clamped-free rotor as shown in figure (1.4). This graph shows how crack may be predicated by frequency change.

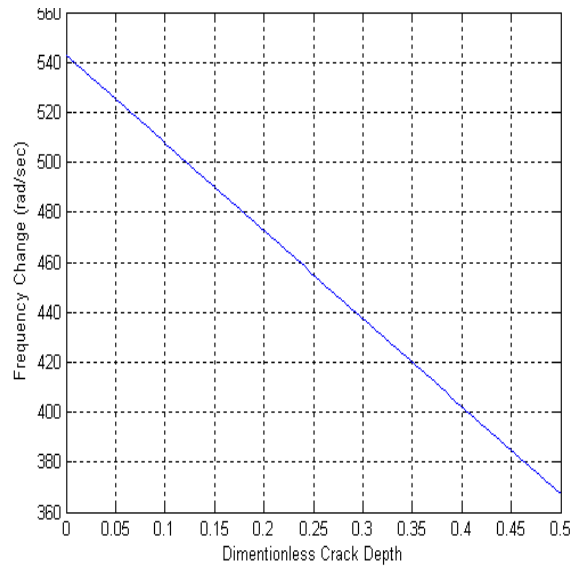


Figure (1.4): frequency change of clamped-free rotor for local model with depth of crack

For each frequency magnitude, given by the four pairs of eigenvalue equation (4.30) forms a liner dependent system of equations. Solving this eigenvalue problem results in the corresponding mode shape or the vector $\{u_x \quad \theta_y \quad u_y \quad \theta_x\}^T$.

The eigenvalues and eigenvectors, or mode shapes, are determined whirl direction to each frequency, and the true natural frequency are plotted versus shaft speed.

Figure (1.4) shows the whirl frequency as a function of shaft speed for crack depths ranging from (0%-30%) of the shaft diameter. The “x” symbols along horizontal axis indicate shaft speeds for which one or more of the eigenvalues has a positive real part, i.e., shaft speeds for which the response is unstable. Two references lines indicating critical speeds and "2x resonance" shaft speed are also include in each figure.

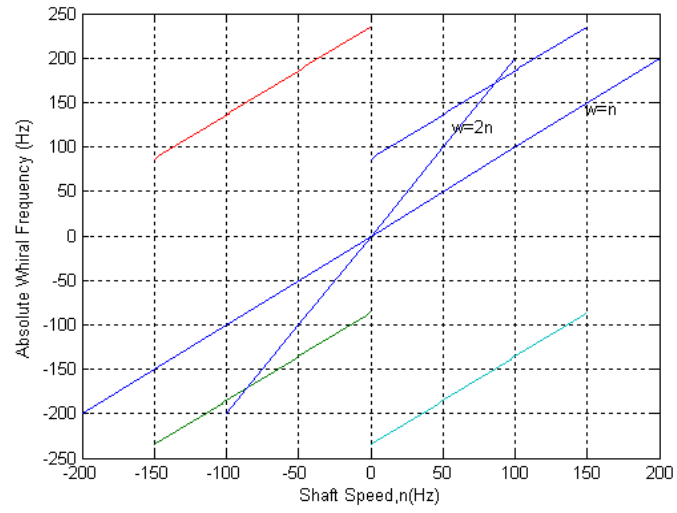


Figure: (1.4a), uncracked

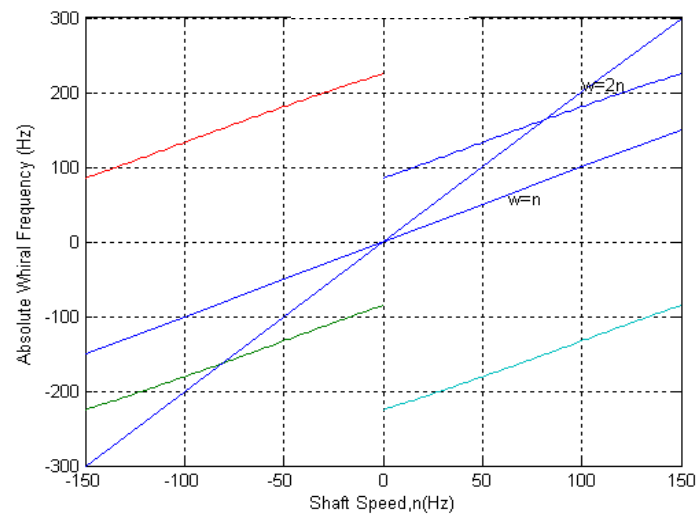


Figure: (1.4b), %10

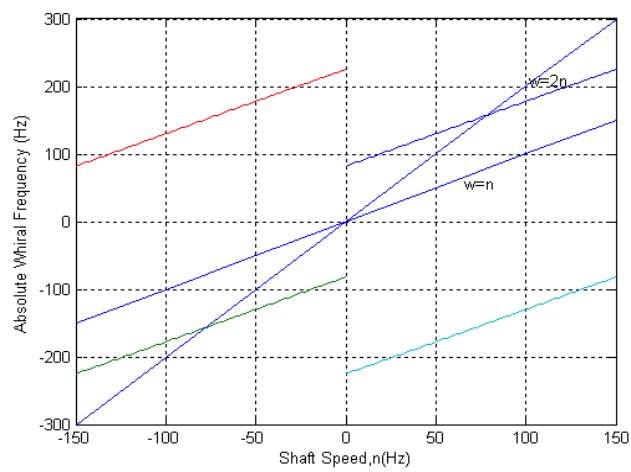


Figure: (1.4c), %20

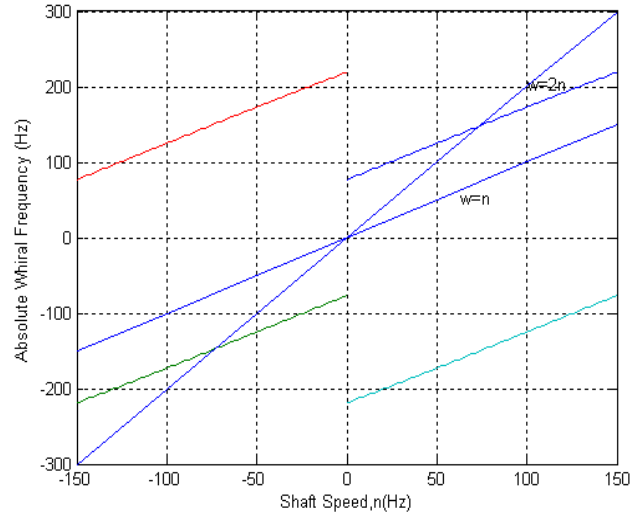


Figure: (1.4d),

Figure (4.10-a-b-c-d) Local Asymmetry Model Free Response at Various Crack Values for Clamped-Free

From this analysis, shaft speeds at which the 2x resonance is maximum can be predicted for various crack depths. Table (1.2) gives the predicted 2x resonance shaft speeds based on the local asymmetry crack model. The decrease in the 2x resonance shaft speeds indicates the decrease in the natural frequency of the system resulting from the flexibility increased by the presence of the crack. This free response analysis of the system containing the local asymmetry crack model indicates that a decrease in natural frequency, which may be observed in primary and secondary critical speeds, is a characteristic of the system response that can be directly attributed to the presence of a transverse crack. Also, these results plotted as can be shown in figure (1.5).

Table (1.2): Resonance Shaft Speeds for Clamped-Free rotor, Local Asymmetry Crack Model

% Crack depth	Resonance Shaft Speed Hz
uncracked	86
10	81.5
20	78.9
30	77.7

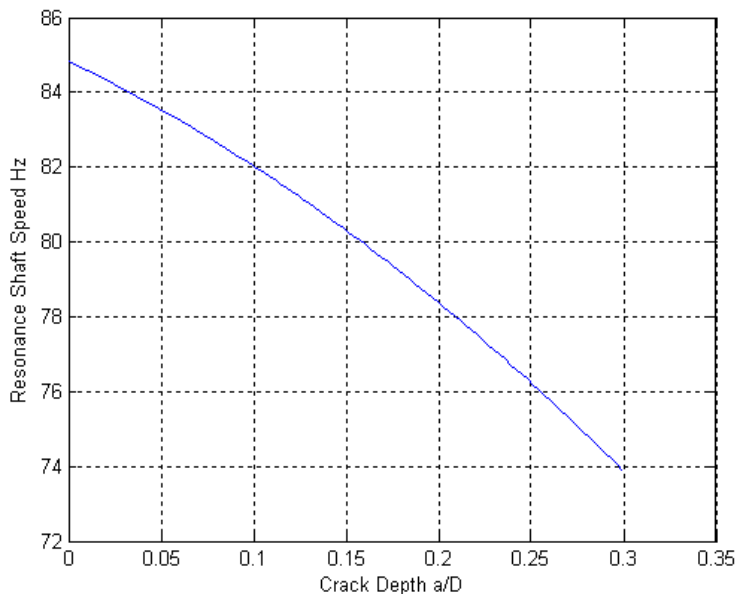


Figure (1.5) Resonance Shaft Speed versus Crack Depth for Clamped-Free Rotor, Local Model



The results obtained from current research for clamped-free rotor, local model compared with the results of the research presented by Sekhar, A. S., (2004) as shown in table below.

Table (1.3) comparison of resonance shaft speed between current research and Sekhar research

%Crack depth	Current research	Research of Sekhr, A. S (2004)	%error
uncracked	86	86	0
10	81.5	78.2	0.033
20	78.9	70	0.089
30	73.7	54.3	0.1189

This comparison shows adequate agreement between these results

CONCLUSIONS

Crack monitoring was discussed for a clamped – free rotor and simply-supported rotor. It was observed that as crack introduced into the rotor, a drop in the natural frequencies occurred. Therefore, the major observation and conclusion can be summarized as follow:

- The behavior of the 2x harmonic component of the system response is effective target observation for a monitoring system where include an increase in magnitude for increasing crack depth as well as a decrease in the shaft speed at which the 2x harmonic component of the system response is maximum as in figures (1.4 and 1.7).
- The presence of a transverse shaft crack has also been shown to induce an unstable response for some shaft speeds as in figure
- The detection of the changes in the magnitude of the 2x harmonic component of the system response becomes much more difficult for shaft speed which is greater than 2x resonance speeds.
- The Transfer matrix method offered a successfully procedure to represented rotating system model and can be used to detect the crack which significantly reduces the flexibility of the rotor.
- It is possible to detect crack in rotor using measurements of change in the natural frequency without need for any analysis as in figures (1.4and 1.6).

REFERENCES

- A.S. Lee and I. Green, 1994, "Rotor dynamics of a mechanical face seal riding on a flexible shaft", ASME Journal of Tribology, 116(2): 345-351.
- E. C. Pestel and F. A. Leckie., 1963, "Matrix Methods in Elastomechanics," McGraw-Hill Book Company, Inc.
 - Nikpour, K. and Dimarogononas, A., 1988, " Local Compliance of Composite Cracked bodies," Composite science and Technology, 32(3), 209-223.
 - Sekhar, A.S. , 2004, "Detection and Monitoring of cracks in a Cross-Down Rotor Supported on Fluid Bearings, "Tribology International", Vol. 37, No. 3, 279-287.